

Chimia 52 (1998) 163–166
 © Neue Schweizerische Chemische Gesellschaft
 ISSN 0009–4293

Geometry Optimization and Excited States of Tris(2,2'-bipyridine)ruthenium(II) Using Density Functional Theory^{a)}

Matthieu Buchs and Claude Daul*

Abstract. During the last two decades, many investigations have been performed on molecules belonging to the family of tris(2,2'-bipyridine)ruthenium(II). In this work, a theoretical approach of the $[\text{Ru}(\text{bpy})_3]^{2+}$ complex using Density Functional Theory and in particular the Amsterdam Density Functional (ADF) program package, is presented. The geometry of the $[\text{Ru}(\text{bpy})_3]^{2+}$ complex has been optimized using the local density approximation (LDA). The optimization has been made within D_3 symmetry and it leads to good agreement with the X-ray structure. As the photochemical and photophysical data suggest, two sets of low-lying empty molecular orbitals are found. In a first study, we dealt with the first set of levels, which correspond to Metal-to-Ligand Charge-Transfer states (MLCT), and calculated the positions of these MLCT states as well as the intensities of the transitions, using the Generalized Gradient Approximations (GGA). The results obtained are in good agreement with the experiment. In a second part, we focus on the upper set of unoccupied orbitals, which are metal-centered. Thus, we calculated the energy of the transition corresponding to the Lowest Ligand Field state, which has been suggested to be responsible for the photoracemization and photosubstitution.

1. Introduction

The $[\text{Ru}(\text{bpy})_3]^{2+}$ complex has certainly been one of the molecules most extensively studied for the last two decades [1–4]. Ru^{II} with polypyridine ligands are still playing a key role in the development of photochemistry, photophysics, photocatalysis, and more. In spite of these numerous studies, there remain unresolved problems [5] in understanding some features of this complex: *e.g.*, the assignments of the lowest excited states and the understanding of the photosubstitution or photora-

cemization. This study has been carried out with Density Functional Theory (DFT), which has emerged over the past decade as a powerful and versatile computational method [6].

2. Method

The ADF [7–9] program package has been employed in all the calculations. The *Vosko, Wilk, and Nusair* [10] (VWN) functional for exchange and correlation energies was used in the Local Density Approximation (LDA). The nonlocal corrections using the *Becke* [11] exchange and *Perdew* [12] correlation (GGA or Generalized Gradients Approximation) have been used in all gradient corrected calculations. We used a set of basis functions present in the program database. All atoms were described by a triple- ζ STO basis set, and the core electrons of $\text{Ru}(1s-3d)$, $\text{N}(1s)$, and $\text{C}(1s)$ were kept frozen. The convergence criteria in the geometry optimizations were set to $1e-3$ Hartree for the changes in energy, $1e-2$ Hartree/Å for the energy gradient, and $1e-2$ Å for the changes between old and new bond lengths.

To evaluate the intensities of optical transitions, we calculated transition dipole moments using the Dipole 1.1 program which rests on the MOs calculated by ADF.

3. Theory

3.1. Energies of Excited States

Before presenting results on excited states, we should describe very briefly how to calculate the energy of these excited states and the intensity of the transitions. Following the proposition of *Ziegler* and coworkers [13], we can replace the energy of a single determinant by the corresponding *statistical* energy as obtained in the DF theory.

The main problem is that we cannot, in general, express the individual multiplet state arising from an open-shell configuration (as it is usually the case in excited states) by a single determinant. Following results from *Daul* [14], it is possible to fully exploit the symmetry in order to simplify the relation between the multiplet splitting and the single-determinant energies. We can then write the multiplet wavefunction

$$\Psi_i = |\alpha\Gamma m_\Gamma S m_S\rangle$$

as a sum of single determinants

$$\Psi_i = \sum_{\mu} A_{i\mu} \phi_{\mu}$$

where

$$\phi_{\mu} = |\chi_1 \chi_2 \chi_3 \dots\rangle$$

is a single-determinant wave function of spin orbitals χ_1, χ_2, χ_3 . It is then possible to write the energy of the multiplet as a weighted sum of single-determinant energies.

3.2. Intensities of the Transitions

Absorption and emission of light originate from the fact that photons and charged particles interact in a way governed by quantum electrodynamics [15]. In this theory, both the particle and the radiation field are described quantum-mechanically. So as to keep things simple, we can describe the radiation field classically, according to the *Maxwell* equations. In this way, the interaction of the field with the particles can best be evaluated by adding a time-dependent perturbation to the *Hamiltonian*, which describes the particles. Then, neglecting the magnetic dipole and the electric quadrupole terms, the proba-

*Correspondence: Prof. C.A. Daul
 Department of Inorganic Chemistry
 and Analytical Chemistry
 University of Fribourg
 Pérolles
 CH-1700 Fribourg
 Tel.: +41 26 300 87 41
 Fax: +41 26 300 97 38
 E-Mail: Claude.Daul@unifr.ch

^{a)} These results were presented as an oral presentation at the Autumn Meeting of the New Swiss Chemical Society (NSCS) in Lausanne, Switzerland, on October 15, 1997.

bility of a transition from an initial state i to a final state f is proportional to

$$W_{if} \propto \left\langle \Psi_i \left| \sum_j r_j \right| \Psi_f \right\rangle^2$$

In the *Born-Oppenheimer* approximation and in the case of a *Franck-Condon* excitation, we may consider only the electronic part of the wavefunction and neglect the overlap factor between the nuclear wavefunctions of the ground and excited states in the upper equation.

Table 1. Comparison Between Calculated and Experimental Structural Parameters of the Ground State of $[\text{Ru}(\text{bpy})_3]^{2+}$ with Atom Labeling in Fig. 1 (distances in Å)

	X-ray [18–20]	LDA	GGA	GGA+Dirac
Ru–N	2.056	2.050	2.099	2.078
N–C(1)	1.355	1.352	1.369	1.368
N–C(5)	1.352	1.336	1.350	1.348
C(1)–C(2)	1.365	1.386	1.400	1.400
C(1)–C(1')	1.475	1.448	1.472	1.470
C(2)–C(3)	1.375	1.380	1.393	1.393
C(3)–C(4)	1.347	1.386	1.397	1.395
C(4)–C(5)	1.362	1.378	1.390	1.391
C(3)–H(3)	0.85	1.094	1.089	1.090
C(4)–H(4)	0.88	1.093	1.090	1.088
C(5)–H(5)	0.88	1.094	1.088	1.087
N–Ru–N'	78.7°	77.9°	76.8°	78.4°
N–C(1)–C(1')–N'	4.67° / 6.6°	7.1°	5.8°	4.5°

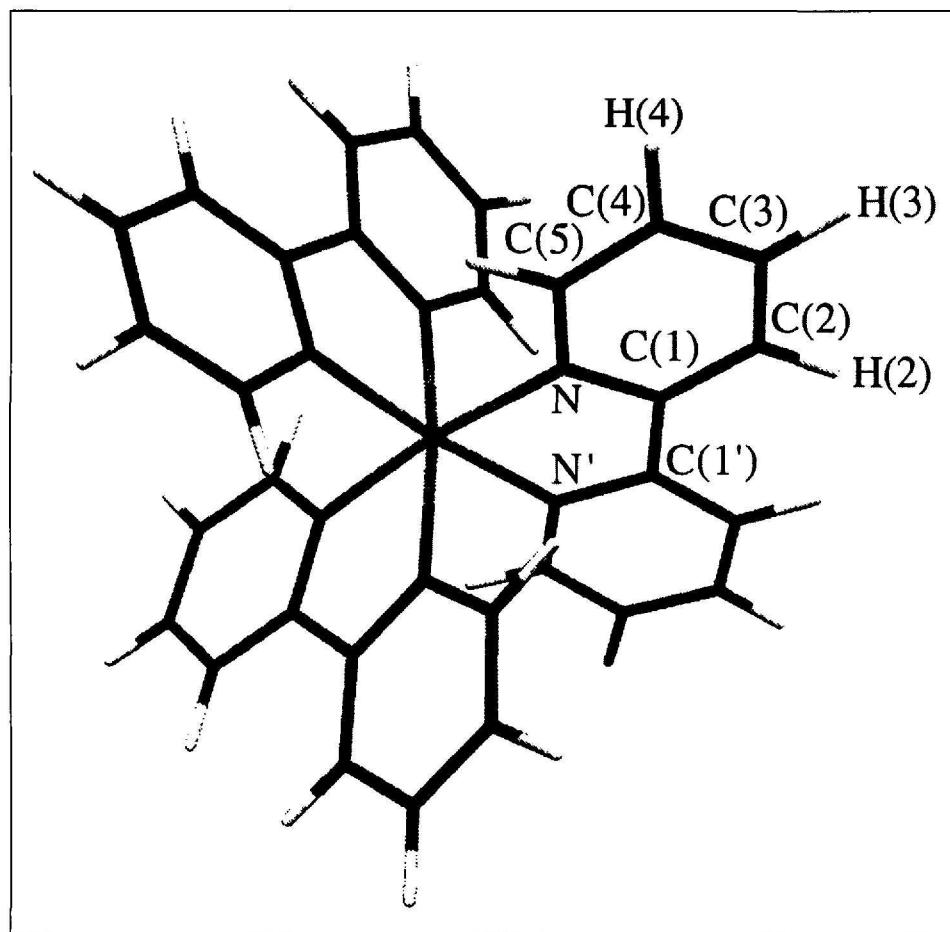


Fig. 1. Molecular conformation of $[\text{Ru}(\text{bpy})_3]^{2+}$ with the atom labeling used in Table 1

4. Results

4.1. Geometry Optimization

As previously mentioned, a great many investigations have been carried on $[\text{Ru}(\text{bpy})_3]^{2+}$, but without prior optimization of the ground-state geometry. We, therefore, performed a DFT calculation to optimize the structure of this complex. In order to reduce the computational effort, we have previously optimized the structure of the bpy ligand in the *cis*-conformation, so as to allow complexation. Table 1 shows that the best results are obtained with the LDA method, especially for the case of the metal-ligand bond length. Our calculations are thus in agreement with the conclusion, often pointed out, that for *Werner* complexes, GGA functionals lead to structural parameters in worse agreement with the experiment than the LDA [16]. When introducing relativistic corrections, we see that the metal-ligand bond length becomes shorter. At a first glance, this is surprising in view of the d-orbital expansion due to the s- and p-orbital contractions. But this particular point has been satisfactorily explained by Ziegler and coworkers [17].

Another interesting feature in the final geometry is the bpy distortion. While the symmetry of the $[\text{Ru}(\text{bpy})_3]^{2+}$ remains D_3 during the optimization, we can see the three-fold axis in Fig. 1, the bpy ligand deviates from planarity, as exhibited by the dihedral angle between the two pyridine cycles of the bpy ligand. This feature has already been observed by X-ray structure determination [18–20]. In these studies, the counterion is not always the same, which makes it difficult to compare the angles. However, the average value of these angles is 4.67° at room temperature and 6.6° at 105 K, as compared with the reasonable angle of 7.1° obtained in our calculation.

4.2. Molecular Orbital Scheme

Despite the fact that there are still unsolved problems in understanding all features of the $[\text{Ru}(\text{bpy})_3]^{2+}$ spectrum, the overall molecular orbital scheme of such a complex is well known, as depicted by Fig. 2.

The highest occupied molecular orbitals, of symmetry a_1 and e , are metal-centered, and the lowest unoccupied molecular orbitals are ligand-centered. Thus, the lowest transitions in the spectrum are of the MLCT type. We found an energy difference, with respect to the ground state, of 18642 cm^{-1} for the lowest 3A_2 and of 19000 cm^{-1} for the lowest 1A_2 excited states, which is in good agreement with

the values 18470 cm^{-1} and 18950 cm^{-1} , respectively, reported in the literature [21] [22]. At higher energies in the molecular orbital scheme, we find an antibonding σ orbital of e symmetry with metal character.

Unlike the geometry optimization, energies of excited states have been obtained using the GGA functional.

4.3. Photochemistry

Although $[\text{Ru}(\text{bpy})_3]^{2+}$ is normally considered as photochemically inert towards ligand substitution, there is increasing evidence that this is not the case. Especially if the pH of the solution and/or the temperature [23] dependence is considered.

As we have seen before in the molecular orbital scheme and in agreement with photophysical and photochemical data, $[\text{Ru}(\text{bpy})_3]^{2+}$ has two sets of unoccupied levels. The lower ones are ligand-centered. These levels are photoinert, whereas the upper set of levels gives rise to ligand-substitution photochemistry and photoracemization. The upper set of levels is metal-centered and exhibits d-orbital parentage.

Van Houten and *Watts* have found experimentally that the upper set of levels, namely the photoactive one, lies 3600 cm^{-1} above the lowest MLCT state [24]. Using the aforementioned method, we have calculated the energy of the lowest d-d transition within the *Franck-Condon* approximation. We obtain a value of $33\,000\text{ cm}^{-1}$ for the energy of the ^3E state, assuming the same geometry as the ground state. There is thus a large difference between the predicted and experimental values for this transition.

We suggest the following explanation for this discrepancy: the initial excitation is a MLCT one. Intersystem crossing (ISC) to a nominal triplet state ($^3\text{MLCT}$) occurs with unit efficiency. Assuming that the photochemical reaction occurs from a set of Ligand Field (LF) levels, there should be a thermal equilibrium between the lowest LF state and the lowest-energy MLCT state. This lowest $^3\text{MLCT}$ state is an extremely long-lived state. It decays with a radiative rate constant of $6.8 \cdot 10^5\text{ s}^{-1}$ and with a radiationless rate constant of $1.22 \cdot 10^6\text{ s}^{-1}$. This feature should allow for vibrational motion, and the difference in energy of 3600 cm^{-1} reported in the literature should not be seen as an absorption following the *Franck-Condon* principle.

A recent work of *Pollak et al.* [25] suggested us to look at the behavior of the MLCT states during the relaxation of the metal-ligand bond length. By a mecha-

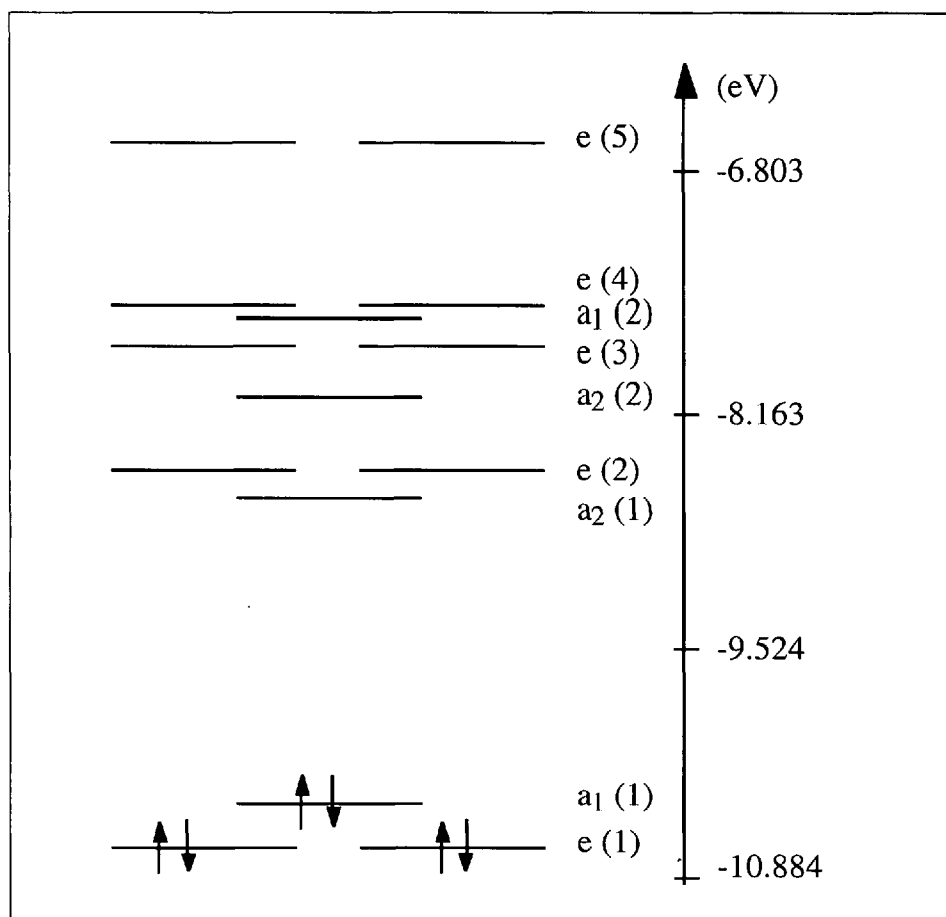


Fig. 2. Molecular orbital scheme of $[\text{Ru}(\text{bpy})_3]^{2+}$ calculated within GGA approximation

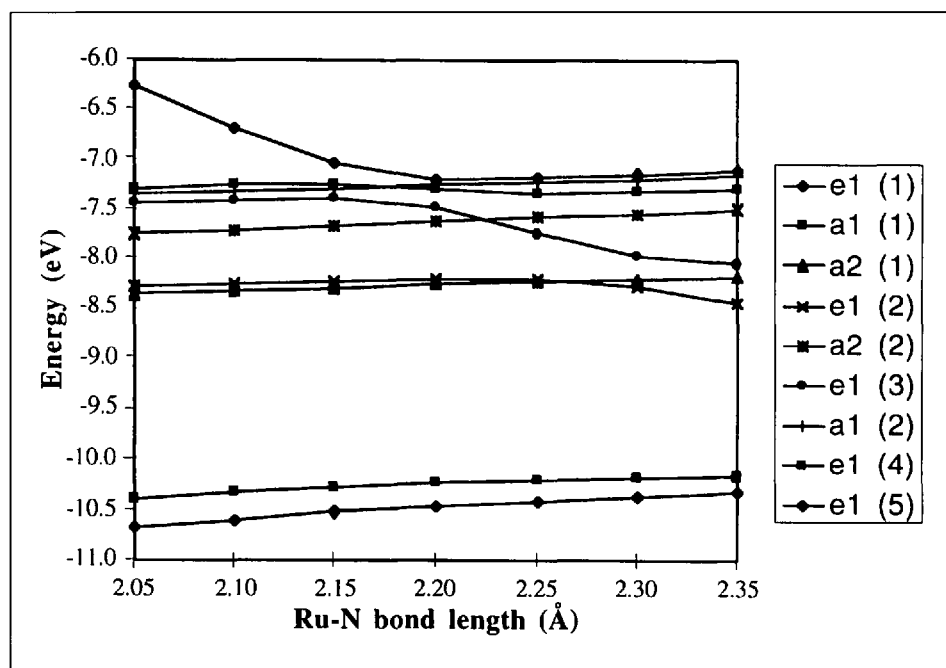


Fig. 3. Energy of the unoccupied orbitals as a function of the metal-ligand bond length

nism of avoided crossing, the metal character of the σ^* orbital in the ground-state geometry is transferred to a π^* orbital of the same symmetry with dominant ligand character, as depicted in Fig. 3.

The result is that the energy of the formal MC transition is lowered with increasing Ru-N bond length, and the resulting state becomes fully dissociative.

Fig. 4 shows the behavior of the excited states when modifying the Ru-N bond length.

5. Conclusion

This work shows again that Density Functional Theory is an efficient tool to

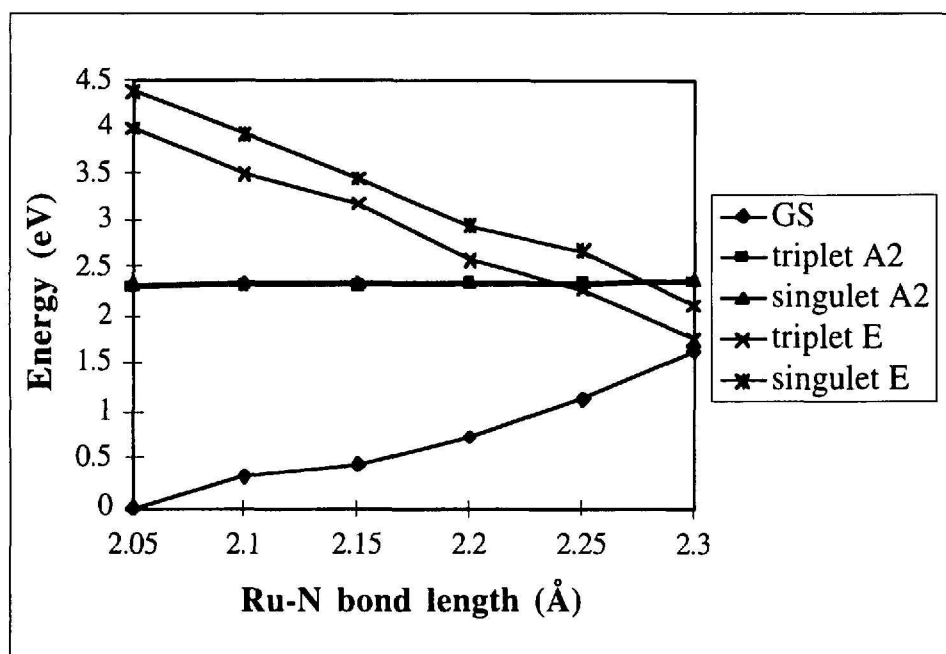


Fig. 4. Energy of the lowest MLCT, lowest dd excited states, and of the ground state as a function of the metal-ligand bond length

Table 2. Orbital Contributions, Calculated within the GGA Approximation

	$d_{x^2-y^2}$	d_{z^2}	d_{xy}	d_{xz}	d_{yz}	$p_x(N)$ $p_y(N)$	$p_z(N)$	$p_x(N)$ $p_y(N)$	$p_z(N)$	Energies (eV)
$e_g(5)$	24%	0%	0%	0%	30%	15%	5%	4%	3%	-6.618
$e_g(5)$	0%	0%	24%	30%	0%	15%	5%	4%	3%	-6.618
$e_g(4)$	1%	0%	0%	0%	1%	10%	8%	46%	34%	-7.306
$e_g(4)$	0%	0%	1%	1%	0%	10%	8%	46%	34%	-7.306
$a_1(2)$	0%	4%	0%	0%	0%	12%	8%	41%	33%	-7.355
$e_g(3)$	1%	0%	0%	0%	2%	6%	3%	45%	39%	-7.430
$e_g(3)$	0%	0%	1%	2%	0%	6%	3%	45%	39%	-7.430
$a_2(2)$	0%	0%	0%	0%	0%	4%	4%	51%	40%	-7.712
$e_g(2)$	4%	0%	0%	0%	5%	15%	8%	31%	30%	-8.282
$e_g(2)$	0%	0%	4%	5%	0%	15%	8%	31%	30%	-8.282
$a_2(1)$	0%	0%	0%	0%	0%	12%	11%	42%	34%	-8.354
$a_1(1)$	0%	79%	0%	0%	0%	1%	1%	11%	2%	-10.324
$e_g(1)$	43%	0%	0%	0%	28%	1%	1%	6%	10%	-10.589
$e_g(1)$	0%	0%	43%	28%	0%	1%	1%	6%	10%	-10.589

apply to transition-metal complexes. In the case of both geometry and lowest MLCT energy, we obtain good agreement with the experiment. Furthermore, we may anticipate that DFT will soon be used understanding unsolved problems, that is, computational chemistry is becoming a tool with predictive value.

We would like to thank Dr. Claudia Stueckl for her contribution. This work has been supported by the Fonds National Suisse de la Recherche Scientifique.

Received: February 18, 1998

- [1] E.H. Kober, T.J. Meyer, *Inorg. Chem.* **1984**, 23, 3877.
- [2] J. Ferguson, F. Herren, *Chem. Phys. Lett.* **1982**, 89, 371.
- [3] J. Ferguson, F. Herren, *Chem. Phys.* **1983**, 76, 45.
- [4] C. Daul, E.J. Baerends, P. Vernooijs, *Inorg. Chem.* **1994**, 33, 3538.
- [5] J.P. Cushing, C. Butoi, D.F. Kelley, *J. Phys. Chem. A* **1997**, 101, 7222.
- [6] T. Ziegler, *Chem. Rev.* **1991**, 91, 651.
- [7] ADF 2.3.0, Theoretical Chemistry, Vrije Universiteit, Amsterdam.

- [8] E.J. Baerends, D.E. Ellis, P. Ros, *Chem. Phys.* **1973**, 2, 41.
- [9] G. te Velde, E.J. Baerends, *J. Comput. Phys.* **1992**, 99, 84.
- [10] S.H. Vosko, L. Wilk, M. Nusair, *Can. J. Phys.* **1980**, 58, 1200.
- [11] A.D. Becke, *Phys. Rev. A: At., Mol., Opt., Phys.* **1988**, 38, 3098.
- [12] J.P. Perdew, *Phys. Rev. B: Condens. Matter* **1986**, 33, 8822.
- [13] T. Ziegler, A. Rauk, E.J. Baerends, *Theor. Chim. Acta* **1977**, 43, 261.
- [14] C. Daul, *Int. J. Quantum Chem.* **1994**, 52, 867.
- [15] H. Eyring, J. Walter, G.E. Kimball, 'Quantum Chemistry', 4th Edn., Wiley, New York-London-Sydney, 1967, p. 107.
- [16] M.R. Bray, R.J. Deeth, V.J. Paget, P.D. Sheen, *Int. J. Quantum Chem.* **1996**, 61, 85.
- [17] T. Ziegler, J.G. Snijders, E.J. Baerends *Chem. Phys. Lett.* **1980**, 75, 1.
- [18] D.P. Rillema, D.S. Jones, H.A. Levy, *J. Chem. Soc., Chem. Commun.* **1979**, 1, 849.
- [19] M. Biner, H.B. Burgi, A. Ludi, C. Rohr, *J. Am. Chem. Soc.* **1992**, 114, 5197.
- [20] D.P. Rillema, D.S. Jones, C. Woods, H.A. Levy, *Inorg. Chem.* **1992**, 31, 2935.
- [21] F. Felix, J. Ferguson, H.U. Güdel, A. Ludi, *J. Am. Chem. Soc.* **1980**, 102, 4096.
- [22] J. Ferguson, E. Krausz, J. Vrbancich, *Chem. Phys. Lett.* **1986**, 131, 463.
- [23] J. Van Houten, R.J. Watts, *Inorg. Chem.* **1978**, 17, 3381.
- [24] J. Van Houten, R.J. Watts, *J. Am. Chem. Soc.* **1976**, 98, 4853.
- [25] C. Pollak, A. Rosa, E.J. Baerends, *J. Am. Chem. Soc.* **1997**, 119, 7324.